

Saturated-Fluorescence Measurements of the Hydroxyl Radical

ROBERT P. LUCHT, D. W. SWEENEY, and N. M. LAURENDEAU

School of Mechanical Engineering, Purdue University, W. Lafayette, IN 47907

Laser-induced fluorescence is a sensitive, spatially resolved technique for the detection and measurement of a variety of flame radicals. In order to obtain accurate number densities from such measurements, the observed excited state population must be related to total species population; therefore the population distribution produced by the exciting laser radiation must be accurately predicted. At high laser intensities, the fluorescence signal saturates (1, 2, 3) and the population distribution in molecules becomes independent of laser intensity and much less dependent on the quenching atmosphere (4). Even at saturation, however, the steady state distribution is dependent on the ratio of the electronic quenching to rotational relaxation rates (4, 5, 6, 7). When steady state is not established, the distribution is a complicated function of state-to-state transfer rates.

The OH radical has been selected for preliminary saturated molecular fluorescence studies. A Nd:YAG pumped dye laser is used to excite an isolated rotational transition, and the resulting fluorescence signal is analyzed both spectrally and temporally in order to study the development of the excited state rotational distribution. It is found that steady state is not established throughout the upper rotational levels, although the directly excited upper rotational level remains approximately in steady state during the laser pulse. The fluorescence signal from the directly excited upper level exhibits considerable saturation.

Frozen Excitation Model

A molecular fluorescence model is presented which is particularly appropriate for short pulse excitation. The frozen excitation model treats the two rotational levels which are directly excited by the laser as an isolated system with constant total number density. Consider the four level molecular model illustrated in Fig. 1. The four level model was solved by Berg and Shackelford (5) for the case where steady state is established throughout all molecular levels. Levels 1e and 2e are the single

0-8412-0570-1/80/47-134-145\$05.00/0

© 1980 American Chemical Society

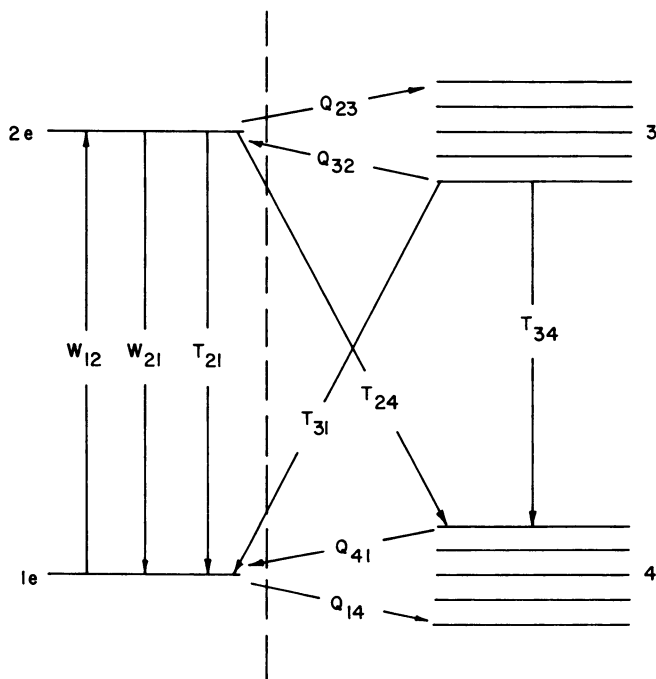


Figure 1. Four-level molecular model. Q_{ij} is the collisional-transfer rate constant from level i to level j , T_{ij} is the sum of the electronic quenching and spontaneous emission rate constants, W_{12} is the absorption rate constant, and W_{21} is the stimulated emission rate constant. W_{12} and W_{21} are proportional to the laser power P_L . The dashed vertical line separates levels $1e$ and $2e$, which are treated as an isolated system, from those levels not affected directly by the laser radiation.

upper and lower rotational levels which are directly connected by the laser radiation. Levels 3 and 4 include the rest of the upper and lower rotational levels, respectively. The rate equations for the level populations N are

$$\dot{N}_1(e) = -N_1(e) [W_{12} + Q_{14}] + N_2(e) [W_{21} + T_{21}] + N_3 T_{31} + N_4 Q_{41}, \quad (1)$$

$$\dot{N}_2(e) = N_1(e) W_{12} - N_2(e) [W_{21} + T_{21} + T_{24} + Q_{23}] + N_3 Q_{32}, \quad (2)$$

$$\dot{N}_3 = N_2(e) Q_{23} - N_3 [T_{31} + T_{34} + Q_{32}], \quad (3)$$

$$N_T = N_1(e)^0 + N_4^0 = N_1(e) + N_2(e) + N_3 + N_4. \quad (4)$$

The superscript 0 refers to level populations prior to laser irradiation. The rate constant notation is described in Fig. 1.

At laser intensities sufficient to saturate the $1e-2e$ transition, the stimulated emission and absorption processes which couple the levels are fast relative to collisional transfer processes, and a quasi-equilibrium balance $[N_2(e)/N_1(e)]_{ss}$ is quickly established. If the total population of levels $1e$ and $2e$ is approximately constant during the laser pulse, the upper level population $N_2(e)$ can be reliably related to $N_1(e)^0$ using an analysis similar to a two level atomic model (1, 2, 3). $\Delta[N_1(e) + N_2(e)]$, the net population transfer into or out of levels $1e$ and $2e$ during the laser pulse, will be nearly zero if the laser pulse length τ_L is less than or comparable to the characteristic collisional transfer time $\tau_c \sim (Q_{23} + T_{24})^{-1} \sim Q_{14}^{-1}$, simply because few collisions will occur during the laser pulse. If $\tau_L > \tau_c$, $\Delta[N_1(e) + N_2(e)]$ will still be much less than $N_1(e)^0$ if the population transfer rate into levels $1e$ and $2e$, $N_3(Q_{32} + T_{31}) + N_4 Q_{41}$, is comparable to the transfer rate out of levels $1e$ and $2e$, $N_1(e) Q_{14} + N_2(e) [T_{21} + T_{24} + Q_{23}]$. This assumption can be justified on the basis of detailed balancing considerations, provided that the rotational relaxation rates in the upper and lower sets of rotational levels are not greatly different. For $\Delta[N_1(e) + N_2(e)] \approx 0$, $N_1(e)^0 = N_1(e) + N_2(e)$ throughout the laser pulse, and Eq. (2) becomes

$$N_2(e) = N_1(e)^0 W_{12} - N_2(e) \{W_{12} + W_{21} + T_{21} + T_{24} + Q_{23} - [N_3/N_2(e)] Q_{32}\}. \quad (5)$$

For a Boltzmann distribution in the upper levels, $N_3 Q_{32} = N_2(e) Q_{23}$. However, for a short laser pulse, level 3 will be significantly underpopulated. Therefore, the factor $[N_3/N_2(e)] Q_{32}$ is negligible compared to Q_{23} .

To show that a quasi-equilibrium ratio $[N_2(e)/N_1(e)]_{ss}$ is established very quickly, Eq. (5) is solved for a step function laser pulse (laser power $P_L = 0$, $t < 0$; $P_L = \text{constant}$, $t > 0$),

$$N_2(e) = N_1(e)^0 W_{12} \tau_{ss} [1 - \exp(-t/\tau_{ss})], \quad (6)$$

American Chemical
Society Library

1155 16th St. N.W.

Washington, D.C. 20036

In Laser Probes for Combustion Chemistry: Crosley, David R.;
ACS Symposium Series; American Chemical Society: Washington, DC, 1980.

$$\tau_{ss} = [W_{12} + W_{21} + T_{21} + T_{24} + Q_{23}]^{-1} \quad (7)$$

At near saturation conditions for OH, $\tau_{ss} < 10^{-10}$ s. Thus, after approximately 100 ps, levels 1e and 2e reach steady state, and $N_2(e)$ is given by

$$N_2(e) = N_1(e)^0 [W_{12}/(W_{12} + W_{21})] [1 + (T_{21} + T_{24} + Q_{23})/(W_{12} + W_{21})]^{-1} \quad (8)$$

At full saturation Eq. (8) becomes

$$N_2(e) = N_1(e)^0 [W_{12}/(W_{21} + W_{12})] = N_1(e)^0 [1 + g_1(e)/g_2(e)]^{-1}, \quad (9)$$

where $g_1(e)$ and $g_2(e)$ are the rotational degeneracies for levels 1e and 2e. Steady state is established much more slowly throughout the rest of the levels via a succession of collisional transfers. For a short laser pulse, $\dot{N}_3 \neq 0$; hence, N_3 cannot be reliably related to a lower level population.

$N_1(e)^0$ is related to N_T by

$$N_T = N_1(e)^0 + N_4^0 = N_1(e)^0 / F_{1B}''(e), \quad (10)$$

where $F_{1B}''(e)$ is the Boltzmann fraction for level 1e. Level 1e can be chosen so that $F_{1B}''(e)$ is a weak function of temperature (8). Consequently, if fluorescence is observed only from level 2e and the flame temperature can be estimated, N_T can be calculated using a simple two level analysis (1, 2, 3).

Experimental System and Results

Fluorescence is induced by a Molelectron Nd:YAG pumped dye laser. The laser repetition rate is 10 Hz, the bandwidth is ~0.01 nm, and the maximum pulse energy and peak power at 309 nm are 3 mJ and .5 MW, respectively. The laser is focused into the flame by a 15 cm focal length lens; the focused spot size is about 100 μ m, as determined from burn patterns on thermal paper. A mirror is placed past the focusing lens to reflect the beam vertically into the flame and parallel to the spectrometer slits. The fluorescence is collected by a 10 cm focal length lens and focused onto the entrance slit of a Spex 1800-II spectrometer operated in second order. The spectral resolution is ~0.1 nm. A 1P28 photomultiplier wired for fast response (9) (rise time \approx 2 ns) is placed at the exit slit. The photomultiplier signal is processed by a Tektronix 5S14N sampler in a 5440 mainframe. The fluorescence spectrum is analyzed by fixing the sampling window of the oscilloscope at a given point in the pulse waveform and scanning the spectrometer; the temporal behavior of fluorescence from individual lines is investigated by setting the spectrometer at the appropriate wavelength and scanning the sampler across the pulse waveform.

The isolated $Q_1(4)$ line of the (0,0) band of the $A^2\Sigma^+ - X^2\Pi$ electronic transition of OH is directly excited by the laser. To

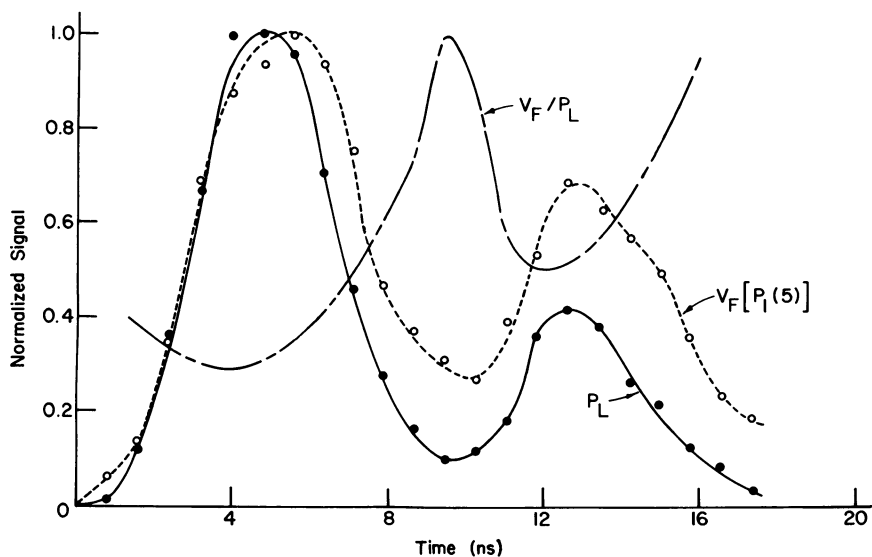


Figure 2. Normalized laser pulse and fluorescence signal from the directly excited upper level vs. time. The laser is tuned to the $Q_1(4)$ line (308.42 nm) and fluorescence is observed from the $P_1(5)$ line (310.21 nm). The laser-pulse energy and peak power are 0.63 mJ and .13 MW, respectively: (---), the ratio of the fluorescence signal to laser power.

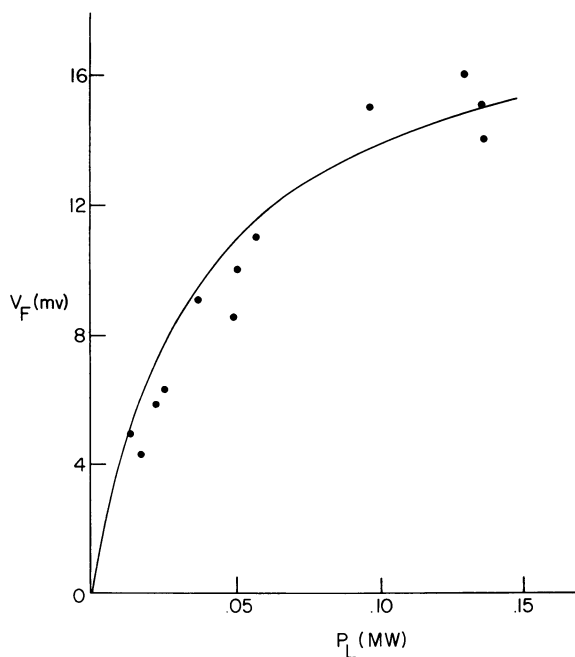


Figure 3. Fluorescence signal vs. laser power. Data was obtained from the curves in Figure 2; points were taken near the peaks and dips of the pulse waveforms: (—), a curve fit through the data using Equation 8.

observe fluorescence from the directly excited $J' = 4.5$, $N' = 4$ upper rotational level, the spectrometer is tuned to the $P_1(5)$ line. Fig. 2 illustrates typical experimental results. The peaks and dips of the laser pulse and the fluorescence pulse nearly coincide; this indicates that a quasi-equilibrium between the directly excited upper and lower rotational levels is established very quickly. When fluorescence power is plotted versus laser power, the fluorescence signal exhibits considerable saturation, as shown in Fig. 3.

The fluorescence spectrum is found to be markedly non-Boltzmann and sharply peaked at the directly excited level throughout the laser pulse. This is due to two effects: the competition between electronic quenching and rotational relaxation processes (4) and the short length of the laser pulse. Because the pulse is so short, steady state is not established throughout the upper rotational levels. The peaks of the fluorescence pulses from levels which are not directly excited by the laser lag the laser pulse peaks by one to four nanoseconds, depending on the energy gap between the given level and the directly excited level.

Using the frozen excitation model to analyze the data shown in Fig. 3, and calibrating the system via Rayleigh scattering (8), a total OH number density of $4 \times 10^{16} \text{ cm}^{-3}$ was calculated for an assumed flame temperature of 2000 K in the methane-air torch. N_T was not compared directly with the results of absorption studies; future flat flame burner studies will involve direct comparison of absorption and fluorescence.

Acknowledgements

We are indebted to Dr. Fred E. Lytle and his students for their advice and assistance, and to Dr. Alan C. Eckbreth of the United Technologies Research Center for his many helpful suggestions. This work was supported by DOE Contract ER-78-S-02-4939.

IV. Literature Cited

1. Piepmeier, E., *Spectrochimica Acta*, 1972, 27B, 431.
2. Baronovski, A.P.; McDonald, J.R., *Applied Optics*, 1977, 16, 1897.
3. Daily, J.W., *Applied Optics*, 1975, 15, 955.
4. Lucht, R.P.; Laurendeau, N.M., *Applied Optics*, 1979, 18, 856.
5. Berg, J.O.; Shackleford, W.L., *Applied Optics*, 1979, 18, 2093.
6. Crosley, D.R., Ed., "Laser Probes for Combustion Chemistry," American Chemical Society: Washington, D.C., 1979; p.
7. Daily, J.W. (Crosley, D.R., Ed.), "Laser Probes for Combustion Chemistry," American Chemical Society: Washington, D.C., 1979, p.
8. Eckbreth, A.C.; Bonczyk, P.A.; Verdick, J.F., *Applied Spectroscopy Reviews*, 1978, 13, 15.
9. Harris, J.M.; Lytle, F.E.; McCain, T.C., *Analytical Chemistry*, 1976, 48, 2095.

RECEIVED February 1, 1980.